Observation of Quantized Motion of Rb Atoms in an Optical Field

P. S. Jessen,[a] C. Gerz, P. D. Lett, W. D. Phillips, S. L. Rolston, R. J. C. Spreeuw, and C. I. Westbrook

National Institute of Standards and Technology, U.S. Department of Commerce, Technology Administration, PHYS A167, Gaithersburg, Maryland 20899

(Received 6 May 1992)

We observe transitions of laser-cooled Rb between vibrational levels in subwavelength-sized optical potential wells, using high-resolution spectroscopy of resonance fluorescence. We measure the spacing of the levels and the population distribution, and find the atoms to be localized to $\frac{1}{15}$ of the optical wavelength. We find up to 60% of the population of trapped atoms in the vibrational ground state. The dependence of the spectrum on the parameters of the optical field provides detailed information about the dynamics of laser-cooled atoms.

PACS numbers: 32.80.Pj, 42.50.Vk

Laser cooling of neutral atoms is typically accomplished in optical molasses, a three-dimensional (3D) configuration of counterpropagating laser beams [1]. This provides a viscous damping of atomic motion, but also gives rise to a periodic optical potential. Since the temperature of atoms in optical molasses can be much less than the depth of the optical potential wells [2,3], one expects a significant fraction of the atoms to be trapped. The observation of strong Dicke narrowing [4] in the fluorescence spectrum of Na in a 3D optical molasses has previously demonstrated that atoms are indeed confined on a subwavelength scale [5]. That spectrum contained no evidence of sidebands, indicating that any bound vibrational levels in the optical potential were not resolved. Since then a calculation [6,7] has predicted that well-resolved vibrational levels can exist in the potential originating from a one-dimensional (1D) molasses, and their detection has been pursued by several groups [8,9]. We have now used fluorescence spectroscopy of ^{85}Rb atoms in a 1D molasses to observe well-resolved sidebands due to spontaneous Raman transitions between vibrational levels. The 1D configuration, along with the nonperturbing nature of fluorescence spectroscopy, allows a straightforward interpretation of the spectrum. A recent, related experiment at ENS, Paris, has observed stimulated Raman transitions between such vibrational levels in the absorption spectrum of a Cs 1D optical molasses [10].

Our 1D optical molasses is realized as follows: A chirp-cooled ^{85}Rb atomic beam is loaded into a 3D magneto-optic trap (MOT) [11] which cools and confines the atoms to a high density. The MOT magnetic field is switched off (time constant ~ 100 μs), leaving a 3D molasses which further cools the atoms to ~ 10 μK. After 1.2 ms the 3D molasses laser is also switched off (switching time < 1 μs). An additional pair of counterpropagating laser beams is continuously present and forms the 1D optical molasses. These beams are 6 mm in diameter with intensities uniform and equal to better than $\pm 10\%$. Because the atoms heat up transversely during the 1D phase, we limit its duration to 1.5 ms and repeat the sequence MOT $\rightarrow$ 3D molasses $\rightarrow$ 1D molasses every 4 ms. The steady-state ^{85}Rb density is on the order of 10^{10} cm^{-3} in a volume of ~ 10 mm^3. The 1D and 3D beams are tuned red of the $5S_{1/2}(F=3) \rightarrow 5P_{3/2}(F'=4)$ transition. An additional laser tuned to the $F=2 \rightarrow F'=3$ transition provides repumping from the $F=2$ hyperfine level.

We use an optical heterodyne technique [5] to measure the fluorescence spectrum. The fluorescence from a 100-μm-diam cylindrical coherence volume is collimated by a lens, passed through a polarization selector, and combined with a local oscillator laser beam on a photodiode. Both the local oscillator and the 1D molasses beams are derived from the same laser, but are frequency shifted by acousto-optic modulators to produce a stable frequency difference of 50 MHz. The power spectrum of the rf signal generated by the photodiode is the power spectrum of the fluorescence mixed down from the laser frequency to 50 MHz. The rf signal is mixed down and filtered, and the spectrum measured by a real-time averaging fast Fourier transform spectrum analyzer with a frequency span of 500 kHz and a resolution of 4 kHz. Data are acquired in 256-μs windows separated by 0.75 ms of signal processing. Two records are acquired during the 1D molasses phase, beginning 150 μs after the 3D beams are extinguished. During the remainder of a sequence the fluorescence is blocked and two additional records are acquired for background subtraction.

In order to approximate a 1D geometry, we detect only fluorescence emitted in a very small (5×10^{-5} sr) solid angle centered within 25–100 mrad of the 1D molasses axis. At smaller angles, the fluorescence is contaminated by scattered light. Residual Doppler broadening arises from atomic motion perpendicular to the 1D axis. It becomes the dominant source of spectral width if the detection angle is larger than 100 mrad, or if the 1D intensity is large enough to cause severe heating in the transverse direction.

The fluorescence spectrum of atoms in 1D molasses depends on the combination of polarizations in the laser beams. In a configuration of orthogonal, linear polarizations (lin$\perp$lin), optical potential wells are created by the

spatially varying polarization. The well depth and the temperature is determined by the light shift, which in the limit of low saturation and large detuning is proportional to $\Lambda = \Omega^2/\Gamma|\Delta|$. Here Ω is the Rabi frequency (assuming a Clebsch-Gordan coefficient of 1) in one of the traveling wave beams making up the 1D molasses, Δ is the detuning from resonance, and Γ is the transition linewidth. A typical spectrum from lin⊥lin molasses is shown in Fig. 1(a). For any detection polarization, it consists of a strong Dicke-narrowed peak at the laser frequency and small sidebands. This spectrum is characteristic of atoms localized to much less than an optical wavelength (the Lamb-Dicke regime). The central peak is due to scattering beginning and ending in the same vibrational level in a well, whereas the sidebands are due to spontaneous Raman scattering between vibrational levels. The red sidebands are more intense than the blue sidebands, indicating a significant population difference from one vibrational level to the next. The observed shape of both the central peak and the sidebands contains a Gaussian contribution from residual Doppler broadening. If Λ and the detection angle are small, this Doppler width is reduced enough that Lorentzian wings of the central peak are evident. For the central peak, we observe full widths at half maximum (FWHM's) in the range from 7 to 20 kHz, while for the first sidebands we observe FWHM's from 10 to 35 kHz.

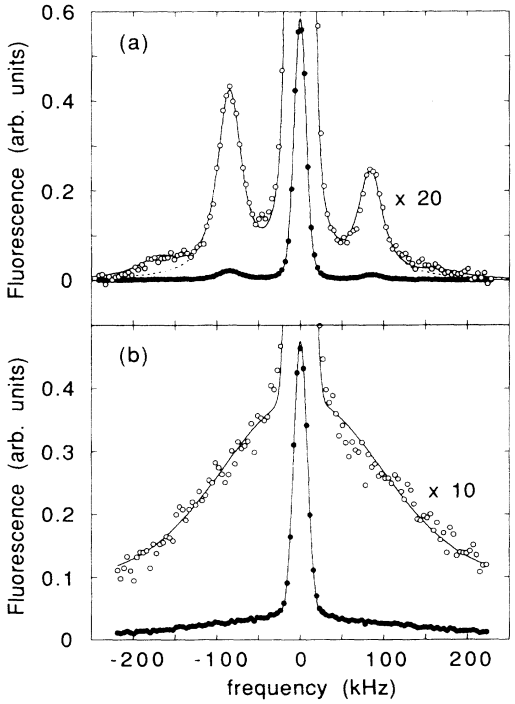

FIG. 1. (a) Fluorescence spectrum of a 1D lin⊥lin molasses for $\Delta = -4\Gamma$ and $\Lambda = 0.23$. The solid line is a fit, including Doppler broadening and the $\Delta v = \pm 2$ sidebands. The dotted line fits only the ± 1 sidebands. (b) Spectrum of a 1D σ^+-σ^- molasses for $\Delta = -4\Gamma$ and $\Lambda = 0.72$. The solid line is a fit by the sum of two Gaussians.

A simple experiment confirms our interpretation of the spectrum of atoms in lin⊥lin molasses. If the central peak and the sidebands are a signature of trapped atoms, they will disappear along with the optical potential wells. For orthogonal circular polarizations in the 1D beams (σ^+-σ^-) the temperature of the atoms is comparable to the lin⊥lin case, but no potential wells are present [3]. A typical spectrum from σ^+-σ^- molasses, with linear detection polarization, is shown in Fig. 1(b). We observe broad (225 kHz) and narrow (20 kHz) components of Gaussian line shape, but no sidebands. The Doppler shift of scattered light is $\mathbf{v}\cdot\Delta\mathbf{k}$, where $\mathbf{v}$ is the atomic velocity and $\Delta\mathbf{k}$ is the change in the wave vector of the light, so the narrow and broad components correspond to scattering in the forward ($\Delta k \approx 0$) and backward ($\Delta\mathbf{k} \approx 2\mathbf{k}$) directions, respectively. As expected, we observe either the broad or the narrow part of the spectrum if we select the appropriate circular polarization for detection.

Cooling and trapping in 1D lin⊥lin molasses is understood [3,12] in terms of optical pumping among ground-state sublevels with spatially varying light shifts caused by the varying ellipticity of the local polarization. A periodic optical potential depending on the polarization is associated with each ground-state sublevel, and the appropriate description is in terms of energy bands [6,7]. We discuss here a simpler physical model of the atomic motion valid near the bottom of the wells [10].

The two linearly polarized traveling waves can be decomposed into two standing waves of σ^+ and σ^- polarization, the nodes of one occurring at the antinodes of the other. The potentials formed by the sum of the two standing waves have minima spaced $\lambda/4$ apart, where the local polarization is either purely σ^+ or σ^-. Consider an atom at an antinode of the σ^+ standing wave. Optical pumping will quickly transfer it to the $m = 3$ state, which has the largest light shift and the deepest potential well. Since the average thermal energy is much smaller than the depth of this well, the atom is unlikely to escape unless it makes a transition to another m state with a shallower potential. Optical pumping out of the $m = 3$ state is strongly suppressed for two reasons. First, the ratio of the squared Clebsch-Gordan coefficients for the transitions $m = 3 \rightarrow m' = 4$ vs $m = 3 \rightarrow m' = 2$ is 28 to 1. Second, the atom is well localized at a node of the σ^- standing wave, and sees very little σ^- light. Consequently, the atoms will spend almost all their time trapped in the wells belonging to either the $m = +3$ or the $m = -3$ state, scattering σ^+ or σ^- light, respectively.

Sidebands in the fluorescence spectrum are due to spontaneous Raman transitions between different vibrational levels. The width of such a Raman transition is determined by the rate of processes transferring population out of the involved levels, such as transitions changing either m or the vibrational quantum number v.

Therefore the Raman width is at least as large as the optical pumping rate out of either of the involved m levels, which for $m \neq \pm 3$ is comparable to the photon scattering rate. Typically this results in a width on the order of 100 kHz. Raman transitions between vibrational levels in the $m = \pm 3$ potentials are narrower, because m-changing transitions are suppressed by the local polarization and the Clebsch-Gordan coefficients, while v-changing transitions are suppressed by the strong spatial localization. Consequently, one expects only transitions with $m = \pm 3$, $\Delta m = 0$, and $\Delta v = \pm 1$ to produce sidebands sufficiently narrow and intense to be easily visible in the spectrum. Transitions with $\Delta v = \pm 2$ are further suppressed by the localization and are just visible in Fig. 1(a).

The central peak of the fluorescence spectrum is due to scattering beginning and ending in the same vibrational level, and its width is not limited by the m- and v-changing transitions that broaden the sidebands [13]. It does, however, contain a contribution from the rate at which an atom hops between wells. As expected, we observe a central peak that is narrower than the sidebands, although residual Doppler broadening and the 4-kHz instrumental resolution make it difficult to determine the intrinsic width.

Consider an atom in the $m = +3$ state, well localized at the antinode of the σ^+ standing wave, and ignore coupling to other ground-state m levels. The optical potential is equal to the light shift, in the limit of low saturation and large, negative detuning given by [3]

$$U = U_0 - (27\hbar\Gamma/112)\Lambda\cos(2kz). \quad (1)$$

Here k is the wave vector of the light, z the position along the 1D axis, and $U_0 = -(29\hbar\Gamma/112)\Lambda$. The numerical factors are due to the Clebsch-Gordan coefficients. Approximating the atomic motion near $z = 0$ with an undamped harmonic oscillator, we find a level spacing

$$\nu_{osc} = \frac{1}{2\pi}\left(\frac{27\hbar k^2\Gamma\Lambda}{28M}\right)^{1/2} = (209\ \text{kHz})\sqrt{\Lambda}, \quad (2)$$

where M is the atomic mass. We expect sidebands in the fluorescence spectrum at a separation $\pm\nu_{osc}$ from the central peak. Figure 2 shows a plot of observed ν_{osc} vs $\Lambda^{1/2}$. From a least-squares fit we determine an experimental constant of proportionality of 167 ± 10 kHz, with an uncertainty primarily associated with the measurement of the absolute intensity in the molasses beams. We have calculated the band structure in the low intensity, large detuning limit, following Ref. [7]. The potential supports 5 to 10 bands, and we find a constant of proportionality in (2) of 184 kHz. The correction is mainly due to the potential's anharmonicity. A direct calculation of the fluorescence spectrum is in progress and may resolve the remaining small discrepancy.

The asymmetry between red and blue sidebands shows the quantum nature of the motion. In the harmonic approximation, the measured constant of proportionality between ν_{osc} and $\Lambda^{1/2}$ completely describes the potential, and we can calculate the relative rates of $\Delta v = \pm 1$ Raman transitions [14] corresponding to the blue and red sidebands. The transition strengths are identical for the Raman transitions $v \rightarrow v+1$ and $v+1 \rightarrow v$, so the difference in strengths of the sidebands is due to the population difference between adjacent levels; this has previously been observed in ion trapping [15]. Assuming a thermal distribution of harmonic oscillator states, the ratio of signal strengths of the first blue and red sidebands is given by the Boltzmann factor $\exp(-h\nu_{osc}/k_B T)$, and we can extract T from the relative areas of the sidebands in the spectrum. Figure 3 shows a plot of this T vs Λ. From 1D theory as well as 3D experiments [16,17], one expects approximate proportionality between T and Λ, which is indeed observed. We observe a minimum temperature of 2 μK, with 60% of the population of the atoms in the vibrational ground state. This analysis ignores the contribution of untrapped atoms, which we expect to be small in most cases [7]. The slope of the fitted line in Fig. 3, as well as the minimum temperature, is roughly a factor of 3 lower than what is observed by time-of-flight (TOF) methods in 3D ^{85}Rb molasses for the same Λ per beam. A significant difference may be expected, since the total

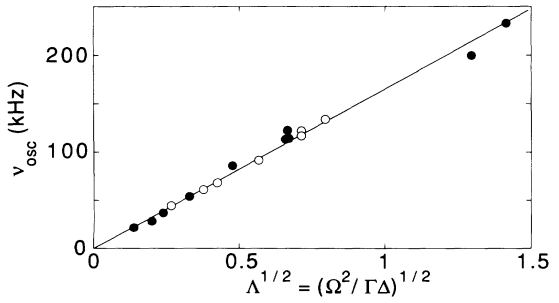

FIG. 2. Measured splitting between sidebands and central peak, as a function of $\Lambda^{1/2}$. Solid circles represent data for $\Delta = -4\Gamma$; open circles, data for $\Delta = -8\Gamma$. The line is a fit of $\nu_{osc} = a\Lambda^{1/2}$.

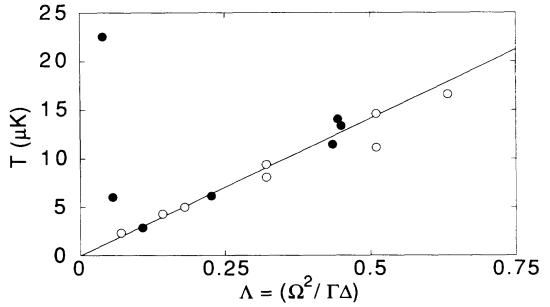

FIG. 3. Measured temperature as a function of Λ. Solid circles represent data for $\Delta = -4\Gamma$; open circles, data for $\Delta = -8\Gamma$. The line is a fit of $T = a\Lambda$ to all the data, omitting the two points with the smallest Λ. The sharp rise in temperature for small Λ is due to a breakdown of laser cooling (see Ref. [12]).

saturation due to all beams as well as the nature of the polarization gradients is different in 3D. Note that a TOF temperature measurement includes the zero point energy of the vibrational ground state.

Using the measured ν_{osc} and T in combination with the harmonic oscillator approximation, we can calculate the ratio of signal strength in the central peak to the sum of the strengths of the sidebands [14]. We find a ratio of approximately 10:1, in reasonable agreement with our data. We can also use the measured ν_{osc} and T to determine x_{rms}, the rms spread of the atomic wave packet. We find $x_{rms}=\lambda/15$, almost independent of Λ due to the simultaneous variation of ν_{osc} and T.

With up to 60% of the population in the vibrational ground state, a trapped atom begins to approximate a minimum uncertainty wave packet. This suggests interesting experiments with driven atomic motion: production of superpositions of vibrational states corresponding to a coherent, oscillating atomic wave packet, or even a squeezed atomic state. It may also be possible to employ sideband-cooling schemes using stimulated and spontaneous Raman transitions between vibrational levels.

We are indebted to the group of C. Cohen-Tannoudji at ENS for sharing their insights in Ref. [10] prior to publication. We thank D. Wineland as well as the rest of the laser cooling group at NIST, Gaithersburg, for helpful discussions. C.G. thanks the Alexander-von-Humboldt Foundation, and R.S. the Niels Stensen Stichting for financial support. This work was partially supported by the U.S. Office of Naval Research.

[a]Permanent address: Institute for Physics and Astronomy, University of Aarhus, 8000 Aarhus C, Denmark.

[1] S. Chu *et al.*, Phys. Rev. Lett. **55**, 48 (1985).
[2] P. Lett *et al.*, Phys. Rev. Lett. **61**, 169 (1988).
[3] J. Dalibard and C. Cohen-Tannoudji, J. Opt. Soc. Am. B **6**, 2023 (1989).
[4] R. Dicke, Phys. Rev. **89**, 472 (1953).
[5] C. I. Westbrook *et al.*, Phys. Rev. Lett. **65**, 33 (1990).
[6] Y. Castin and J. Dalibard, Europhys. Lett. **14**, 761 (1991).
[7] Y. Castin, Ph.D. thesis, Université Paris VI, 1992 (unpublished).
[8] R. Gupta *et al.*, Bull. Am. Phys. Soc. **37**, 1139 (1992).
[9] D. Grison *et al.*, Europhys. Lett. **15**, 149 (1991).
[10] P. Verkerk *et al.*, Phys. Rev. Lett. **68**, 3861 (1992).
[11] E. Raab *et al.*, Phys. Rev. Lett. **59**, 2631 (1987).
[12] Y. Castin, J. Dalibard, and C. Cohen-Tannoudji, in *Light Induced Kinetic Effects in Atoms, Ions and Molecules*, edited by L. Moi *et al.* (ETS Editrice Pisa, Pisa, 1990).
[13] J. Cooper and R. J. Ballagh, Phys. Rev. A **18**, 1302 (1978).
[14] D. J. Wineland and W. M. Itano, Phys. Rev. A **20**, 1521 (1979).
[15] F. Dietrich *et al.*, Phys. Rev. Lett. **62**, 403 (1989). In this work the atom was probed by absorption rather than emission, yielding a stronger *blue* sideband.
[16] P. D. Lett *et al.*, J. Opt. Soc. Am. B **6**, 2023 (1989).
[17] C. Salomon *et al.*, Europhys. Lett. **12**, 683 (1990).